

Optical feedback dynamics from a mid-infrared single-frequency quantum cascade laser

L. Jumpertz,^{1,2} K. Schires,¹ O. Spitz,¹ M. Sciamanna,⁴ & F. Grillot^{2,3}

¹ LTCI, Télécom ParisTech, Université Paris-Saclay, 46 rue Barrault, 75013 Paris, France

² mirSense, Centre d'intégration NanoINNOV, 8 avenue de la Vauve, 91120 Palaiseau, France

³ Center for High Technology Materials, University of New-Mexico, 1313 Goddard SE, Albuquerque, NM 87106, United States

⁴ LMOPS, CentraleSupélec, Université de Lorraine, 57070 Metz, France.

grillot@telecom-paristech.fr

Résumé. Les lasers à cascade quantique sont des sources semiconductrices basées sur des transitions intersous-bandes au sein de la bande de conduction. Pouvant émettre sur une large plage de longueurs d'onde allant du moyen infra-rouge au terahertz, ils sont devenus une source privilégiée pour des applications telles que la spectroscopie de gaz, les communications en espace libre ou les contre-mesures optiques [?]. L'objectif du travail est d'étudier numériquement l'évolution du diagramme de bifurcation en fonction de trois paramètres clés : le courant de pompe, la longueur de la cavité externe et le facteur d'élargissement spectral du laser intrinsèque à la structure. L'étude numérique confirme que le scénario de déstabilisation caractérisée par des fluctuations basses fréquences est bien reproductible dans d'autres conditions expérimentales ou sur d'autres types de structures à cascade quantique.

Abstract. Quantum cascade lasers are unipolar semiconductor lasers offering access to wavelengths from the mid-infrared to the terahertz domain and promising impact on various applications such as free-space communications, high-resolution spectroscopy, or optical countermeasures. Unlike bipolar semiconductor lasers, stimulated emission in QCLs is obtained via electronic transitions between discrete energy states inside the conduction band. In this article we conduct a numerical investigation of optical feedback dynamics of quantum cascade lasers by considering three key-parameters : pump current, the external cavity length, and the linewidth enhancement factor. The numerical study confirms that the destabilization scenario characterized by low frequency fluctuations is perfectly reproductible with other experimental conditions or other types of quantum cascade laser structures.

1 Introduction

Quantum cascade lasers (QCLs) are unipolar semiconductor lasers based on intersubband transitions within the conduction band [?]. Mid-infrared (IR) QCLs can now operate in single- or multimode configuration, in pulsed or continuous-wave operation, at room temperature with thermo-electrical cooling, and have therefore become privileged sources for gas spectroscopy, free-space communications or optical countermeasures. QCLs are renowned for their high stability compared to interband laser diodes, in particular when subjected to external phenomena such as optical feedback [?]. In laser diodes, optical feedback, ie. reinjection of part of the emitted light after reflection on a mirror, can destabilize the laser and may lead to a chaotic behavior [?]. On the other hand, no chaos has been observed so far in mid-IR QCLs, even though experimental studies have shown that optical feedback can influence static properties such as laser threshold, output power or wavelength [?]. The analysis of the optical spectra of a distributed feedback (DFB) QCL in several feedback conditions furthermore evidences a set of feedback ratios f_{ext} , defined as the ratio between reinjected and emitted powers, and external cavity length L_{ext} for which the laser becomes unstable. This work aims to numerically study the birth of chaotic dynamics in a mid infrared QCL subjected to optical feedback. Influence of the pump current, the external cavity length and the linewidth enhancement factor are considered.

2 Description of the numerical model

The Lang and Kobayashi equations used to model the impact of optical feedback on the QCL are expressed as follows [?].

$$\frac{dY}{ds} = (1 + i\alpha)ZY + \eta \exp(-i\Omega_0\theta)Y(s - \theta) \quad (1)$$

$$T \frac{dZ}{ds} = P - Z - (1 + 2Z)|Y|^2 \quad (2)$$

where Y is the slowly varying envelop of the electric field and Z the carrier number normalized to the value at threshold. Both equations are normalized with respect to the photon lifetime τ_p , T is the carrier to photon lifetime ratio, θ the normalized external cavity roundtrip time, Ω_0 the normalized laser frequency above threshold, $\bar{P} = I/I_{th}-1$ the bias current over threshold and η the normalized feedback coefficient :

$$\eta = \frac{\tau_p}{\tau_{in}} 2C_l \sqrt{f_{ext}} \quad (3)$$

with τ_{in} the laser cavity roundtrip time. C_l is the coupling strength coefficient at the front facet, whose expression is complex in DFB lasers and depends on facet phases as described in [?]. Finally α is the linewidth enhancement factor. This parameter, defined as the ratio between the real and imaginary parts of the nonlinear susceptibility, is of prime importance in semiconductor lasers since it quantifies the coupling between the phase and amplitude of the electrical field [?]. In the Lang and Kobayashi equations, the carrier to photon lifetime ratio is $T = 0.265$, the normalized bias current is $P = 0.02$, the normalized cavity roundtrip time is $\theta = 492$ and the linewidth enhancement factor is $\alpha = 1.7$, value that best fits the experimental results. The feedback phase $\Omega_0\theta = -atan(\alpha)$ is chosen to an arbitrary value.

3 Results and discussion

The laser under study is a DFB QCL emitting around $5.6 \mu\text{m}$. Its active area in AlInAs/GaInAs was grown on an InP cladding. A high-reflective coating on the back facet and a top metal grating enable single-mode operation in continuous-wave at room temperature. All parameters used in the simulations can be found elsewhere.

3.1 Bifurcation diagram

The numerical bifurcation diagram is shown in Figure ???. The stable solution appearing for low feedback ratios destabilizes at the Hopf point $f_{ext} = 2.14\%$ and the route to chaos does not involve any oscillations at the characteristic frequency, only oscillations at the external cavity frequency. The bubble of chaos that occurs between $f_{ext} = 2.69\%$ and $f_{ext} = 2.91\%$ takes the form of LFF that are superimposed on the external cavity frequency oscillations. Finally, at high feedback ratios, the QCL is stable again on a different external cavity mode with larger output power. Running the simulation by decreasing the feedback ratio instead of increasing it gives another solution of successive stable external cavity modes, which coexist with the periodic and chaotic solution found previously. This multistability is difficult to observe experimentally since it requires a very fine tuning of the feedback ratio. Moreover, since the basin of attraction of the LFF dynamics is large, as shown numerically, it captures most of the system trajectories in phase space. The numerical bifurcation diagram therefore unveils a class A-like scenario in the QCL under optical feedback, without any oscillations at the laser characteristic frequency.

3.2 Influence of the α -factor

As shown in Figure ??, the destabilization of the QCL under optical feedback still occurs for lower values of α -factor, and the bifurcation scenario remains the same, involving oscillations at the external

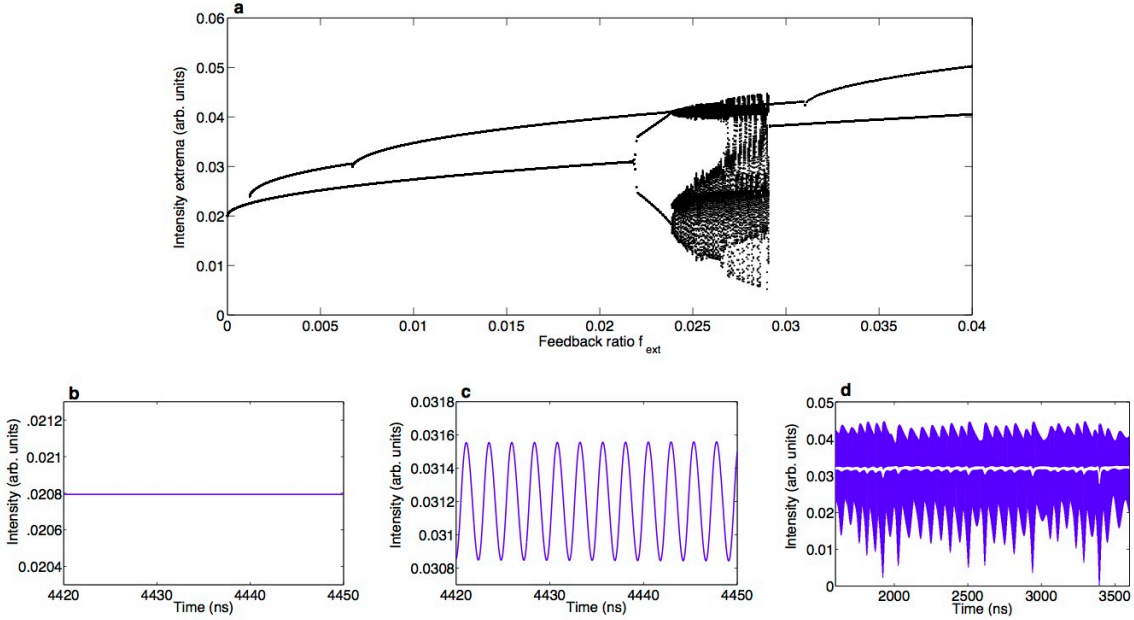


Figure 1. Numerical bifurcation diagram for $P = 0.02$ and $L_{ext} = 35$ cm, and associated time series. a) Numerical bifurcation diagram. b) Time trace for $f_{ext} = 0.11\%$, showing stable signal. c) Time trace for $f_{ext} = 2.14\%$, showing oscillations at the external cavity frequency. d) Time trace for $f_{ext} = 2.59\%$, showing both LFF and oscillations at the external cavity frequency.

cavity frequency and low frequency fluctuations. However, the feedback ratio at which the first Hopf bifurcation occurs increases drastically for smaller LEF, and the amplitude of the LFF area is strongly reduced. For instance, when $\alpha = 1$, with the same parameters $P = 0.02$ and $L_{ext} = 35$ cm, the Hopf bifurcation takes place at $f_{ext} = 75\%$ and the LFF, which appear around $f_{ext} = 80\%$, disappear after an increase in feedback ratio of only 0.05% . Such high values of feedback ratios are obviously unreachable experimentally. In THz QCLs, for which α -factor values much lower than 1 were reported, there will probably be no occurrence of chaos.

3.3 Influence of the bias current

As expected from the study in interband lasers, the appearance of LFF depends strongly on the bias current, and they are rapidly displaced towards high feedback ratios as the pump parameter P increases. For $L_{ext} = 35$ cm and $\alpha = 1.7$, the first Hopf bifurcation occurs at $f_{ext} = 2.14\%$ at $P = 0.02$ and at $f_{ext} = 26.44\%$ for $P = 0.10$, whereas the LFF appear at $f_{ext} = 2.69\%$ and $f_{ext} = 29.34\%$ respectively, as shown in Figure ??.

3.4 Influence of the external cavity length

As presented in Figure ??, the feedback ratio at which the Hopf point occurs shows only a small variation when increasing the external cavity length from 25 to 55 cm (blue circles), whereas the LFF begin at a significantly lower feedback ratio (2.15% for 55 cm instead of 2.76% for 25 cm, red diamonds), and the amplitude of the LFF area also decreases (yellow squares representing the limit of restabilization). This trend is also similar to that obtained from the analysis of the optical spectra, where the extend of

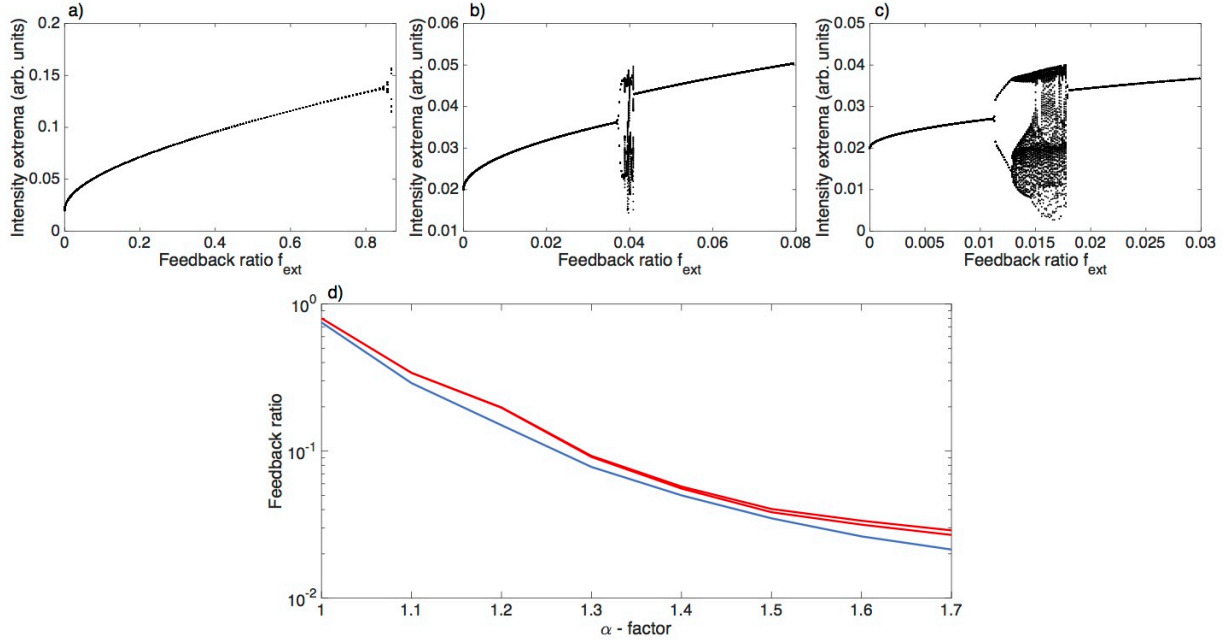


Figure 2. Influence of the α -factor on the bifurcation diagram for $P = 0.02$ and $L_{ext} = 35$ cm. a) Numerical bifurcation diagram for $\alpha = 1$. b) Numerical bifurcation diagram for $\alpha = 1.5$. c) Numerical bifurcation diagram for $\alpha = 2$. d) Evolution of the Hopf point (in blue) and of the lower and upper limits of the LFF area (in red) as a function of the α -factor.

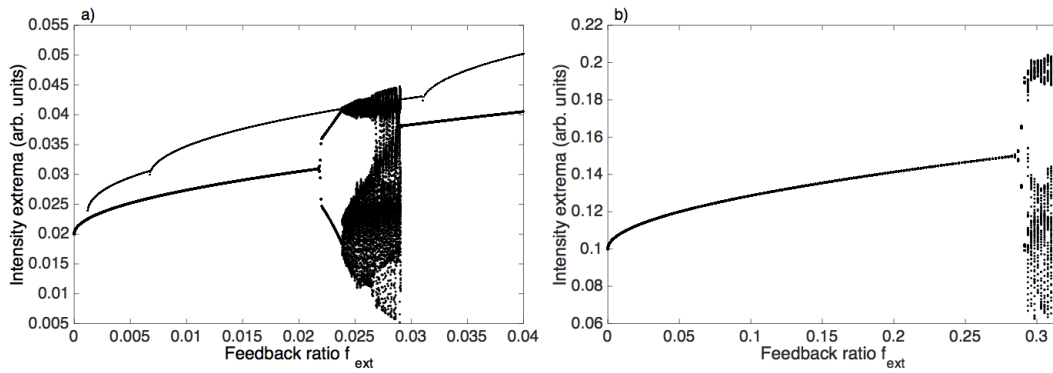


Figure 3. Influence of the bias parameter P on the bifurcation diagram for $L_{ext} = 35$ cm and $\alpha = 1.7$. a) Numerical bifurcation diagram for $P = 0.02$. b) Numerical bifurcation diagram for $P = 0.10$.

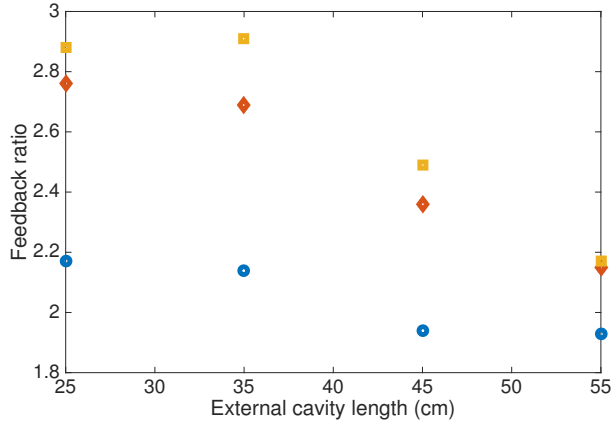


Figure 4. Influence of the external cavity length L_{ext} on the bifurcation diagram for $P = 0.02$ and $\alpha = 1.7$. In blue circles, occurrence of the first Hopf bifurcation. In red diamonds, appearance of the LFF. In yellow squares, restabilization.

the fourth regime, which is supposed to correspond to instabilities and chaos, decreases rapidly with the external cavity length, although its starting point remains roughly the same.

Finally, for some configurations, a second destabilization was observed numerically for high feedback ratios (higher than what is experimentally achievable), resulting in periodic or multi-periodic oscillations. However, no second chaotic bubble was obtained with the considered parameters. The same conclusions on the class A-like dynamics of QCLs subject to optical feedback, with chaos that may appear very close to threshold, have been recently obtained by analytic resolution of the full set of equations of a QCL under optical feedback [?].

4 Conclusions

In this work, we have numerically investigated the optical feedback dynamics of a mid-IR QCL. Under certain feedback conditions, the QCL can become chaotic and follow a route to chaos similar to that observed in class A lasers, with a destabilization taking place at the external cavity frequency and deterministic chaos characterized by LFFs. Simulations have shown that for lower α -factor values, the feedback ratio corresponding to the Hopf point is much higher, while the amplitude of the LFF regions is drastically reduced. The chaotic bubble also occurs for smaller feedback rates when increasing the cavity length while the Hopf bifurcation increases when the pump current gets larger. The possible appearance of chaos in QCLs has several consequences. First, this leads to a generalization of the use of mid-IR optical isolators in experimental setups and in packaged QCLs in order to avoid parasitic optical feedback on the laser. On the other hand, a chaotic QCL could be used in new experiments based on chaos, similarly to those existing in the near-IR. We could imagine mid-IR chaotic communications, based on chaos modulation for encryption and synchronized chaos for message transmission [?], chaotic LIDAR [?] or unpredictable sources for optical countermeasures.

Acknowledgments : This work is funded by the Direction Générale de l'Armement (DGA).

Références